

LEP PRECISION ELECTROWEAK MEASUREMENTS FROM THE Z^0 RESONANCE

David Strom*

University of Oregon, Eugene, Oregon 97403

Representing the ALEPH, DELPHI, L3, and OPAL Collaborations, and the
LEP Energy Working Group

ABSTRACT

Preliminary electroweak measurements from the LEP Collaborations from data taken at the Z^0 resonance are presented. Most of the results presented are based on a total data sample of 12×10^6 recorded Z^0 events which included data from the 1993 and 1994 LEP runs. The Z^0 resonance parameters, including hadronic and leptonic cross sections and asymmetries, τ polarization and its asymmetry, and heavy-quark asymmetries and partial widths, are evaluated and confronted with the predictions of the Standard Model. This comparison incorporates the constraints provided by the recent determination of the top-quark mass at the Tevatron. The Z^0 resonance parameters are found to be in good agreement with the Standard Model prediction using the Tevatron top-quark mass, with the exception of the partial widths for Z^0 decays to pairs of b and c quarks.

*Supported by DOE Contract DE-FG06-85ER40224.

1 Introduction

The LEP measurements of the Z^0 resonance parameters allow precision tests of the Standard Model to be made in a number of ways. The prediction of the top-quark mass from radiative corrections to processes at the Z^0 resonance is perhaps the most notable. The prediction of the top-quark mass from the Z^0 resonance parameters has recently become a test with the discovery and subsequent determination of top-quark mass from the Tevatron.^{1,2} The addition of a constraint from the top-mass measurement allows measurements of the Z^0 resonance parameters to provide a first glimpse at what the mass of the Higgs boson might be. Other interesting tests of the Standard Model are made by forming ratios of quantities where radiative corrections which depend on the unknown Higgs mass largely cancel. These ratios, which include $R_{inv} = \Gamma_{inv}/\Gamma_{l+l-}$, $R_b = \Gamma_{b\bar{b}}/\Gamma_{had}$, and $R_c = \Gamma_{c\bar{c}}/\Gamma_{had}$, are ideal for searching for physics beyond the Standard Model. In the context of the Standard Model, the ratio $R_\ell = \Gamma_{had}/\Gamma_{l+l-}$ provides a precise measurement of the strong coupling constant α_s .

2 Theory Review

This section reviews the essentials of electroweak theory needed for understanding measurements of the Z^0 resonance parameters in unpolarized electron–positron annihilation. A more complete review of electroweak theory is given elsewhere in these proceedings.³

At tree level, only three inputs are needed to calculate electroweak quantities. These three inputs are typically taken to be the electromagnetic coupling constant, α_{em} , the Fermi Constant, G_F , and the Z^0 mass, m_Z . Calculations of higher-order corrections require that the masses of the fermions, the mass of the Higgs boson, and the strong coupling constant, α_s , also be known. Almost all radiative corrections involving the light quarks can be absorbed into the value of the electromagnetic coupling constant, α_{em} , by using a “running” value of this constant. (For more details, see Ref. 3.) For this report, we take⁴ $\alpha_{em}(m_Z^2) = 1/128.896 \pm 0.090$ where the error (largely due to uncertainties in the measured total cross section for electron–positron annihilation at low energies) is propagated through all of the fit results reported in Sec. 8. The uncertainty on G_F is too small to influence the final results.

After correcting for the purely electromagnetic effects of initial state radiation, and ignoring the effects of final state photon and gluon radiation, the cross section for electron–positron annihilation to fermions at the Z^0 can be written as:

$$\begin{aligned} \frac{2s}{\pi\alpha_{em}(m_Z^2)^2 N_c} \frac{d\sigma}{d\cos\theta} = & \\ & q_f^2 (1 + \cos^2\theta) \\ & - 8Re\{\chi(s)q_f(g_{ve}g_{vf}(1 + \cos^2\theta) + 2g_{ae}g_{af}\cos\theta)\} \\ & + 16|\chi(s)|^2[(g_{ve}^2 + g_{ae}^2)(g_{vf}^2 + g_{af}^2)(1 + \cos^2\theta) + 8g_{ve}g_{ae}g_{vf}g_{af}\cos\theta], \end{aligned} \quad (1)$$

where q_f is the fermion charge, g_{vf} and g_{af} are the vector and axial vector fermion couplings, N_c is the color factor, $\alpha_{em}(m_Z^2)$ is the value of the electromagnetic coupling constant at the Z^0 resonance, and

$$\chi(s) = \frac{G_F m_Z^2}{8\pi\alpha_{em}(m_Z^2)\sqrt{2}} \frac{s}{s - m_Z^2 + is\Gamma_Z/m_Z}, \quad (2)$$

where m_Z and Γ_Z are the mass and width of the Z^0 . The first term in Eq. (1) is from photon exchange, the next term from interference between the Z^0 and photon exchange, and the third term from Z^0 exchange. Near the Z^0 peak, the third term dominates; in most of the following, the photon term and the interference term have been set to their Standard Model values.

The effects of radiative corrections can be seen by expressing the partial widths for the Z^0 to fermion pairs as

$$\Gamma_{f\bar{f}} = \frac{G_F m_Z^3}{6\pi\sqrt{2}} (g_{af}^2 + g_{vf}^2) (1 + \delta_{QCD}) N_c (1 + \delta_{QED}). \quad (3)$$

Here, δ_{QED} reflects the effects of final state photon radiation, δ_{QCD} the effects of final state QCD corrections, and N_c a color factor. The δ_{QED} is almost negligible, but for quark pairs $\delta_{QCD} = \frac{\alpha_s}{\pi} + \dots$ is substantial. The additional radiative corrections can be absorbed into the definition of g_{af} and g_{vf} . At tree level, these quantities are given by

$$\begin{aligned} g_{vf_{tree}} &= I_3 - 2q_f \sin^2\theta_W \\ g_{af_{tree}} &= I_3, \end{aligned} \quad (4)$$

where q_f and I_3 are the charge and weak isospin of the fermion. If the radiative corrections are absorbed into the definition of g_{af} and g_{vf} , we then *define* the effective value of $\sin^2\theta_W$ for leptons as

$$\sin^2\theta_{eff}^{lept} \equiv \frac{1}{4}\left(1 - \frac{g_{v\ell}}{g_{a\ell}}\right). \quad (5)$$

In the context of the Improved Born Approximation,⁵ the radiative corrections which affect both g_{vf} and g_{af} can be described by the ρ parameter as follows:

$$\begin{aligned} g_{vf} &= \sqrt{\rho}(I_3 - 2q_f \sin^2\theta_{eff}^{lept}) \\ g_{af} &= \sqrt{\rho}(I_3). \end{aligned} \quad (6)$$

Note that the effect of radiative corrections to the asymmetries are determined by $\sin^2\theta_{eff}^{lept}$, while the total and partial widths of the Z^0 depend primarily on ρ . The effect of the top and Higgs mass on ρ are substantial, making the total width Z^0 sensitive to these quantities. This dependence is illustrated taking

$$\rho = 1 + \Delta\rho_{top} + \Delta\rho_{Higgs} \quad (7)$$

where $\Delta\rho_{top} \simeq 3\frac{G_F}{8\pi^2\sqrt{2}}m_t^2$ and $\Delta\rho_{Higgs} \simeq -11\frac{G_F m_Z^2 \sin^2\theta_w}{24\pi^2\sqrt{2}} \ln \frac{m_H^2}{\cos^2\theta_w m_Z^2}$. New physics may affect the values of $\sin^2\theta_{eff}^{lept}$ and ρ in different ways, making it important to make accurate measurements of both the asymmetries and the partial and total widths of the Z^0 .

It is possible to construct quantities which have reduced or altered dependence on the top and Higgs mass by taking the ratio of widths. In the absence of new physics, we can determine α_s from

$$R_l \equiv \frac{\Gamma_{had}}{\Gamma_{l+l-}} = \frac{N_{had}}{N_{l+l-}}, \quad (8)$$

where l refers to any charged lepton. N_{had} and N_{l+l-} are the acceptance-corrected number of multihadrons and lepton pairs. The radiative corrections to this quantity are dominated by the $1 + \delta_{QCD}$ factor in Γ_{had} . The ratio R_l does have a slight top-mass dependence from $\sin^2\theta_{eff}^{lept}$, and from nonuniversal corrections to $\Gamma_{b\bar{b}}$, which are discussed below. The remaining radiative corrections are the same for Γ_{had} and Γ_{l+l-} . Another similar quantity is the total hadronic cross section at the peak of the Z^0 resonance defined by

$$\sigma_{had}^{pole} \equiv \frac{12\pi}{m_Z^2} \frac{\Gamma_{ee}\Gamma_{had}}{\Gamma_Z^2}. \quad (9)$$

This quantity is determined from the acceptance-corrected number of hadronic events, and the measured luminosity determined from small-angle Bhabha scattering. Again, most of the radiative correction to the partial widths cancel in the ratio. Since both Γ_{had} and Γ_Z depend on α_s , the dependence of σ_{had}^{pole} on α_s is 40% of that of R_l .

The quantity with the least dependence on the top and Higgs mass is

$$R_{inv} \equiv \frac{\Gamma_{inv}}{\Gamma_{l+l-}} = \frac{\Gamma_Z - \Gamma_{had} - 3\Gamma_{l+l-}}{\Gamma_{l+l-}}, \quad (10)$$

which can be used to search for new “invisible” particles which couple to the Z^0 and to check that the couplings for neutrinos correspond to the Standard Model predictions.

The ratios $R_b = \Gamma_{b\bar{b}}/\Gamma_{had}$ and $R_c = \Gamma_{c\bar{c}}/\Gamma_{had}$ are also good places to look for new physics. R_b has some sensitivity to the top mass; vertex corrections involving top quarks give R_b a quadratic correction of approximately 2%, for a top mass of 180 GeV. Before the measurement of the top-quark mass at the Tevatron, this dependence was useful for determining the top-quark mass without an assumption about the Higgs mass. Now that the top-quark mass has been determined directly, the measurement of R_b constitutes a direct test of the Standard Model.

To probe the ratio of vector to axial vector couplings of the Z^0 to quarks and leptons, the forward–backward asymmetries are measured. The asymmetry due to the Z^0 exchange is given by

$$A_{fb} \equiv \frac{3}{4} \mathcal{A}_e \mathcal{A}_f = \frac{N_{forward} - N_{backward}}{N_{forward} + N_{backward}} \quad (11)$$

where

$$\mathcal{A}_f \equiv \frac{2g_{vf}g_{af}}{(g_{vf})^2 + (g_{af})^2} = \frac{2g_{vf}/g_{af}}{1 + (g_{vf}/g_{af})^2}. \quad (12)$$

The measured asymmetries must be corrected for the residual effects of the $Z^0 - \gamma$ interference, and in the case of electrons, for t-channel γ exchange. The polarization of the outgoing τ leptons may also be used as a probe of the ratio of vector and axial vector couplings of the leptons. For the unpolarized beams available at LEP, the τ polarization is given by

$$P_\tau(\cos\theta) \equiv \frac{\sigma_{right} - \sigma_{left}}{\sigma_{right} + \sigma_{left}} = -\frac{\mathcal{A}_\tau + \mathcal{A}_e \frac{2\cos\theta}{1+\cos^2\theta}}{1 + \mathcal{A}_\tau \mathcal{A}_e \frac{2\cos\theta}{1+\cos^2\theta}}. \quad (13)$$

3 LEP Luminosity and Energy Calibration

The results presented in the following sections are based on data collected at LEP by the ALEPH, DELPHI, L3, and OPAL Collaborations. Various improvements to the LEP machine have increased both the peak luminosity and the general reliability so that in 1994, a typical experiment was able to record 55 pb^{-1} of data. The amount of data taken on and off peak is tabulated below in Table 1. In most cases, the data from 1992 and before has been fully analyzed. However, almost all of the results based on the 1993 and 1994 data are *preliminary*.

Year	On Peak	Off Peak
'90	4 pb^{-1}	3 pb^{-1}
'91	8 pb^{-1}	5 pb^{-1}
'92	24 pb^{-1}	
'93	13 pb^{-1}	18 pb^{-1}
'94	55 pb^{-1}	
Total	104 pb^{-1}	26 pb^{-1}

Table 1: Recorded luminosity for a typical LEP experiment.

The electroweak analysis here benefits from the large amount of data taken at energy points approximately 1.8 GeV above and below the Z^0 resonance. Measurements of the Z^0 mass, m_Z , and the total width of the Z^0 , Γ_Z , depend primarily on the amount of data taken off peak, and on the energy calibration of the LEP machine.

The energy calibration of the LEP machine for 1993 has now been finalized,⁷ and the error in the LEP energy scale contributes approximately 1.4 MeV to the systematic error on m_Z and 1.5 MeV to the systematic error on Γ_Z . The beam energy is determined by allowing transverse polarization to build up in the electron or positron beam, and then using resonant depolarization to determine the beam energy. The systematic error on individual resonant depolarization measurements is approximately 1.1 MeV.

The measurements of the beam energy must be then transported from the time of the resonant depolarization to the time at which the data were taken. Significant changes in the energy occur due to tidal distortions of the LEP ring. Because the

length of the beam orbit is fixed by the RF system, distortions in LEP's shape will cause the beams to travel slightly off center in quadrupole magnets and shift the beam energy. Because of the strong focusing employed in the LEP machine, a 1 MeV shift in the beam energy corresponds to an average shift in the quadrupoles of only $13 \mu\text{m}$. Calculations of the effect of the tidal variation of the beam energy agree well with repeated measurements made in dedicated tide experiments. The results of these experiments are shown in Fig. 1.

Additional variations in the machine energy are seen on much longer time scales. Measurements of the beam orbit indicate that the distortions in the LEP ring are possibly due to changes in the ground water level and the level of Lake Geneva. The extrapolation from the time of the resonant depolarization measurements to the time of data-taking contributes the dominant systematic error in Γ_Z and m_Z . Other effects which are important in the energy calibration can be found in Ref. 7.

The results presented here do not include data taken in the 1995 LEP scan which is expected to include about 18 pb^{-1} per experiment of off-peak data. This scan has more frequent energy calibrations, including some at the start of fills. This will allow a reduction of the systematic error associated with slow distortions in the LEP shape.

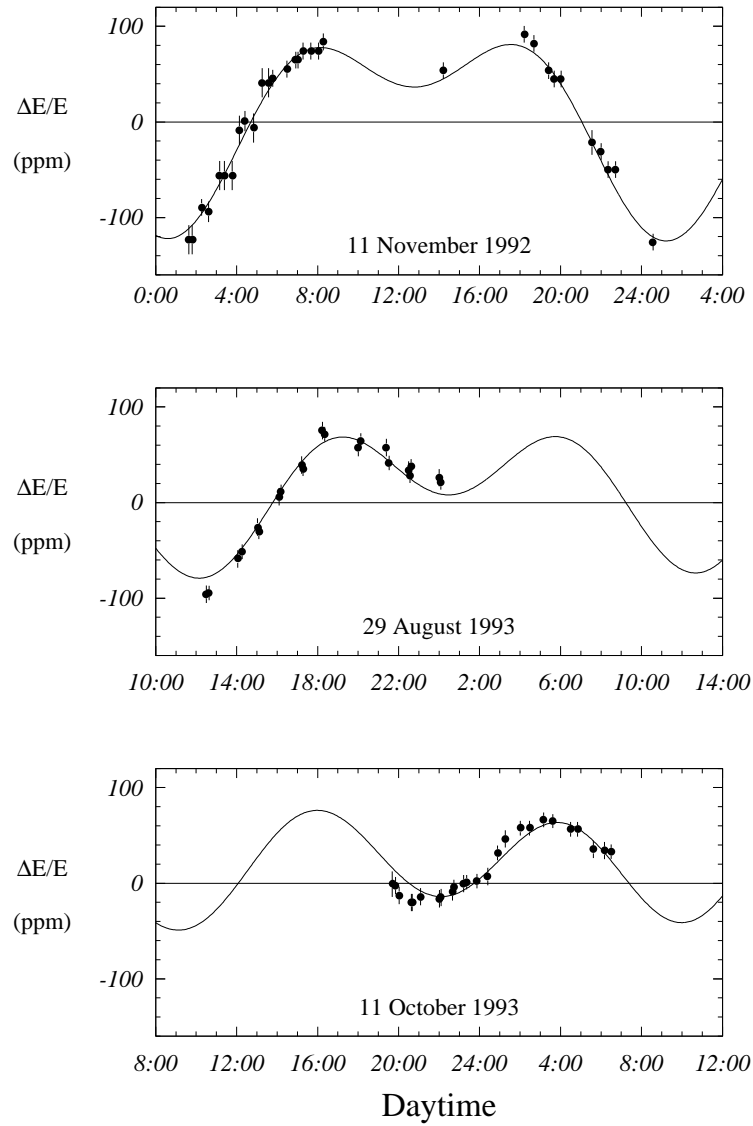


Figure 1: Results of dedicated tide experiments. The beam energy measured with resonant depolarization has been corrected for changes of the integrated dipole field. The solid line shows the prediction of the tidal model. Adapted from Ref. 7.

4 Line-Shape Measurements

The line shape of the Z^0 is measured using decays of the Z^0 to hadrons and leptons. The hadronic decays comprise the largest sample and give us the most information about Γ_Z and m_Z . These events are separated from the beam-related background, the background from the process $e^+e^- \rightarrow e^+e^-X$ and leptonic decays of the Z^0 , using a selection based on charged and neutral multiplicity, energy balance, and total energy. The decays of the Z^0 to electron and muon pairs are identified by requiring high total energy and the presence of identified electrons and muons. Decays of the Z^0 to τ pairs are separated from the hadronic decays on the basis of multiplicity, and from the other lepton pairs on the basis of missing energy. Details of the selection procedures used by the LEP Collaborations can be found in Refs. 8–11.

For the determination of m_Z and Γ_Z , it is only necessary to know the relative efficiency and backgrounds of the off-peak energy points to on-peak points. These relative acceptances are generally known with a greater precision than the corresponding statistical errors. For measurement of the absolute cross sections, it is necessary to have an absolute luminosity measurement and a calculation of the absolute acceptances. In general, it has been possible to reduce the systematic error on the luminosity and the hadronic and leptonic acceptances considerably beyond what had been anticipated at the start of the LEP operation.

The experimental and theoretical luminosity measurement has been dramatically improved. Previous to the operation of LEP, luminosity measurements at the 1% level were rare. Now that a second generation of luminosity monitors are in use at LEP, the typical experimental systematic error has been reduced to below 0.1%. The theoretical error is currently 0.16% (Ref. 12), and further improvement is perhaps possible. The detailed breakdown of the experimental systematic errors is given in Table 2. When combining measurements, it has been assumed that the experimental systematic errors in these acceptances are uncorrelated. The leptonic acceptances are 0.15% to 0.8%, and are similar to the corresponding statistical errors. The error in the hadronic acceptance is at the 0.1% level, which is slightly larger than the corresponding statistical error.

The individual LEP Collaborations extract values for the parameter set m_Z , Γ_Z , R_ℓ , σ_{had}^{pole} , and the lepton forward-backward asymmetries, A_{FB} , by fitting the measured cross section and asymmetries as a function of energy using the program

	ALEPH		DELPHI		L3		OPAL	
	'93 prel.	'94 prel.	'93 prel.	'94 prel.	'93 prel.	'94 prel.	'93 prel.	'94 prel.
$\mathcal{L}^{exp.}$	0.087%	0.116%	0.21%	0.09%	0.12%	0.15%	0.076%	0.079%
σ_{had}	0.073%	0.073%	0.13%	0.15%	0.08%	0.2%	0.15%	0.16%
σ_e	0.50 %	0.48%	0.44%	^(a)	0.3%	0.4%	0.23%	0.24%
σ_μ	0.25 %	0.26%	0.28%	0.40%	0.3%	0.6%	0.16%	0.15%
σ_τ	0.34 %	0.32%	0.8%	^(a)	0.8%	1.5%	0.43%	0.46%

Table 2: The experimental systematic errors for the analysis of the Z^0 line shape at the Z^0 peak. The errors quoted do not include the common uncertainty due to the LEP energy calibration. The treatment of correlations between the errors for different years is described in Refs. 8-11. Adapted from Ref. 6.

^(a)No preliminary result quoted yet.

ZFITTER.¹³ For the analysis of the process $e^+e^- \rightarrow e^+e^-$, it is also necessary to correct for the photon t-channel. In the fitting procedure, the correlated uncertainties in the LEP energy scale at the various scan points are taken into account. The result of a nine-parameter fit, which does not assume lepton universality, is given in Table 3. The average values for the parameters shown in Table 4 are obtained by taking into account the correlated uncertainties between the experiments (primarily due to uncertainty in the LEP energy scale) and the theoretical uncertainty in the luminosity calculation. Also shown in Table 4 are the average parameters assuming lepton universality. The results for the individual leptonic channels are in good agreement with the assumption of lepton universality. (Because of the nonzero mass of the τ lepton, a 0.2% difference is expected between R_τ and R_ℓ .)

	ALEPH	DELPHI	L3	OPAL
m_Z (GeV)	91.1924 ± 0.0037	91.1849 ± 0.0034	91.1936 ± 0.0036	91.1852 ± 0.0036
Γ_Z (GeV)	2.4954 ± 0.0057	2.4913 ± 0.0054	2.5022 ± 0.0054	2.4960 ± 0.0053
σ_{had}^{pole} (nb)	41.56 ± 0.09	41.39 ± 0.10	41.48 ± 0.11	41.47 ± 0.10
R_e	20.54 ± 0.11	20.88 ± 0.16	20.89 ± 0.12	20.90 ± 0.10
R_μ	20.88 ± 0.09	20.70 ± 0.09	20.80 ± 0.11	20.796 ± 0.073
R_τ	20.77 ± 0.10	20.61 ± 0.16	20.73 ± 0.17	21.00 ± 0.11
$A_{FB}^{0,e}$	0.0196 ± 0.0044	0.0233 ± 0.0070	0.0125 ± 0.0070	0.0081 ± 0.0051
$A_{FB}^{0,\mu}$	0.0189 ± 0.0029	0.0166 ± 0.0030	0.0168 ± 0.0038	0.0137 ± 0.0027
$A_{FB}^{0,\tau}$	0.0206 ± 0.0039	0.0210 ± 0.0057	0.0287 ± 0.0064	0.0183 ± 0.0035
$\chi^2/\text{d.o.f.}$	181/185	151/135	118/138	10/6 ^(a)

Table 3: Line-shape and asymmetry parameters from nine-parameter fits to the data of the four LEP experiments. Adapted from Ref. 6.

^(a)This parameter set has been obtained from a parameter transformation applied to the 15 parameters of the OPAL fit,¹¹ which treats the γZ^0 interference terms for leptons as additional free parameters. The extra parameters for the γZ^0 interference terms have been fixed to their Standard Model values in the transformation. The $\chi^2/\text{d.o.f.}$ for the 15-parameter fit to the data is 87/132.

Parameter	Average Value	Average Value with Lepton Universality
$m_Z(\text{GeV})$	91.1885 ± 0.0022	91.1884 ± 0.0022
$\Gamma_Z(\text{GeV})$	2.4963 ± 0.0032	2.4963 ± 0.0032
$\sigma_{had}^{pole}(nb)$	41.488 ± 0.078	41.488 ± 0.078
R_e	20.797 ± 0.058	
R_μ	20.796 ± 0.043	
R_τ	20.813 ± 0.061	
R_ℓ		20.788 ± 0.032
$A_{FB}^{0,e}$	0.0157 ± 0.0028	
$A_{FB}^{0,\mu}$	0.0163 ± 0.0016	
$A_{FB}^{0,\tau}$	0.0206 ± 0.0023	
$A_{FB}^{0,\ell}$		0.0172 ± 0.0012
$\chi^2/\text{d.o.f.}$	$36/27$	$39/31$

Table 4: Average line-shape and asymmetry parameters from the data of the four LEP experiments given in Table 3. Also shown is the average of the measurements assuming lepton universality. Adapted from Ref. 6.

5 τ Polarization Measurements

The study of the polarization of τ decays in unpolarized collisions provides additional information about the lepton couplings to the Z^0 . The momentum and angles of the visible τ decay products are used to obtain the average polarization of the τ .

For two-body decays ($\tau \rightarrow h\nu_\tau$), the τ energy spectrum is given by

$$\frac{1}{N} \frac{dN}{dx} \simeq 1 + \xi_s \mathcal{P}_\tau (2x - 1), \quad (14)$$

where $x = E_h/E_{beam}$ and

$$\begin{aligned} \xi_s &= 1 && \text{spinless hadrons } (\pi, K) \\ \xi_s &= \frac{m_\tau^2 - 2m_h^2}{m_\tau^2 + 2m_h^2} && \text{spin one hadrons } (\rho, a_1). \end{aligned} \quad (15)$$

When the τ decays to either a ρ or a_1 , additional information from the subsequent decay of the hadron is used. For three-body final states from leptonic τ decays, the momentum spectrum is given by

$$\frac{1}{N} \frac{dN}{dx} = \frac{1}{3} \left[(5 - 9x^2 + 4x^3) + \mathcal{P}_\tau (1 - 9x^2 + 8x^3) \right]. \quad (16)$$

The main challenge to the experiments is to devise selection criteria for the various τ decay channels that have a well-understood dependence on momentum, and minimize the contamination from other τ decay modes.

From the correlation between angle and polarization, it is possible to extract both \mathcal{A}_e and \mathcal{A}_τ . From examination of Eq. (13), it can be seen that the value of \mathcal{A}_e is determined from the asymmetry of the τ polarization. The uncertainty on \mathcal{A}_e is limited by available statistics. The individual values of \mathcal{A}_τ have a sizable contribution from systematic errors which are roughly equivalent to the statistical errors. These systematic errors are not correlated between experiments. The individual measurements from the LEP experiments are described in Refs. 14–17 and are summarized in Table 5, which is taken from Ref. 6.

6 Heavy-Quark Partial Widths and Asymmetries

Measurements of heavy-quark partial widths and asymmetries are based on hadronic decays of the Z^0 , where it has been possible to tag one or more jets as

	\mathcal{A}_τ	\mathcal{A}_e
ALEPH ('90 - '92) final	$0.136 \pm 0.012 \pm 0.009$	$0.129 \pm 0.016 \pm 0.005$
DELPHI ('90 - '92) final	$0.148 \pm 0.017 \pm 0.014$	$0.136 \pm 0.027 \pm 0.003$
L3 ('90 - '94) prel.	$0.152 \pm 0.010 \pm 0.009$	$0.156 \pm 0.016 \pm 0.005$
OPAL ('90 - '94) prel.	$0.134 \pm 0.010 \pm 0.009$	$0.134 \pm 0.015 \pm 0.004$
LEP Average	0.1418 ± 0.0075	0.1390 ± 0.0089

Table 5: LEP results for \mathcal{A}_τ and \mathcal{A}_e .

containing a heavy quark. To measure the asymmetry, it is also necessary to reconstruct the b- or c-quark direction. The original quark-antiquark axis can be estimated from the event thrust axis, the quark direction from the reconstructed quark charge.

In this section, the tagging techniques are briefly described followed by a discussion of the measurement of R_b and R_c . Next, we discuss the asymmetry measurements. Finally, all of the results are combined using a common set of assumptions about the errors introduced from measurements at lower energies, and other needed input such as degree of b-mixing present at LEP. (Several of the topics related to heavy-quark physics are treated in more detail elsewhere in these proceedings.¹⁸)

6.1 Measurements of R_b and R_c

Hadronic decays of the Z^0 to pairs of b and c quarks can be tagged with a variety of techniques. The relatively long b-hadron lifetime of $c\tau \sim 0.45$ mm, and the large mean charged multiplicity of the b hadron, makes tagging techniques based on the identification of detached vertices attractive.

Another useful technique is based on the weak decays of b and c hadrons to final states including leptons. Leptons from b-hadron decays are separated from those from c decays on the basis of the momentum and transverse momentum of the leptons with respect to the jet axis. Since the transverse momentum of the lepton is a measure of the parent's mass, the large b-hadron mass ensures that the leptons at high transverse momentum are likely to be from b hadrons. The

large b-hadron mass is also exploited by event shape, techniques which are based on the difference between the jet structure of b hadrons and the lighter quarks.

Heavy quarks are also tagged by fully or partially reconstructing c hadrons. The measured momentum of the c hadron, as well as decay length and event-shape information, are used to separate the $c \rightarrow c$ hadron from cascade process $b \rightarrow c \rightarrow c$ hadron.

Recent measurements of $R_b = \frac{\Gamma_{b\bar{b}}}{\Gamma_{had}}$ are based on double-tag techniques that reduce the dependence of the analysis on the tagging efficiency. In a tagging method without background, the total number of tagged jets is given by

$$n_t = 2R_b N_{had} \varepsilon, \quad (17)$$

where ε is the tagging efficiency. The number of double-tagged events is

$$n_{tt} = R_b N_{had} \varepsilon^2. \quad (18)$$

Ignoring any correlations between the tagging efficiencies for the jets in the same event, Eqs. (17) and (18) can be solved, giving

$$R_b = \frac{n_t^2}{4n_{tt} N_{had}}. \quad (19)$$

This expression is independent of the ε , which may have large experimental and theoretical uncertainties. In practice, it is necessary to apply a small correction for correlations between the efficiencies of two jets in the same event. In addition, it is necessary to correct n_t and n_{tt} for contamination from light quarks and charm. The correction for charm contamination is the largest contribution to the error on the individual measurements of R_b and gives the measured value of R_b a dependence on the assumed value of R_c . This dependence is parameterized as

$$R_b = R_b^{measured} + a(R_c) \frac{R_c - R_c^{assumed}}{R_c}, \quad (20)$$

with the value of $a(R_c) \simeq -0.15$ for the three measurements which dominate the average.

The values of the three measurements which dominate the LEP average are shown in Fig. 2, and a summary of the correlated systematic errors is given in Table 6. The correlated uncertainty is dominated by the uncertainty in the relative fraction of charm hadrons produced and the decay multiplicity of the charm hadrons.^{6,28}

	ALEPH shape (Ref. 19)	ALEPH lifetime (Ref. 20)	DELPHI multiple (Ref. 21)	L3 shape (Ref. 22)	OPAL multiple (Ref. 23)
Charm production	0.0	-0.85	-1.0	0.0	-0.94
D^0 lifetime	0.0	-0.28	-0.2	0.0	-0.23
D^+ lifetime	0.0	-0.36	-0.2	0.0	-0.29
D_s lifetime	0.0	-0.22	-0.2	0.0	-0.17
D decay multiplicity	0.0	-0.57	-0.4	0.0	-0.76
BR($D \rightarrow K^0$)	0.0	0.0	+0.6	0.0	+0.59
$g \rightarrow b\bar{b}, c\bar{c}$	0.0	-0.33	-0.2	0.0	-0.46
Long-lived light hadrons	0.0	-0.24	-0.4	0.0	-0.33
BR($c \rightarrow \ell$)	+0.6	0.0	-0.2	0.0	-0.28
Semileptonic model $c \rightarrow \ell$	-2.1	0.0	-0.2	0.0	-0.25
$\langle x_E(c) \rangle$	+0.8	-0.12	-0.4	+1.8	-0.75
Semileptonic model $b \rightarrow \ell$	-1.3	0.0	+0.2	0.0	0.0
$\langle x_E(b) \rangle$	0.0	0.0	0.0	-3.1	0.0
Total corr. error	2.7	1.2	1.5	3.6	1.7

Table 6: Example of breakdown of the correlated systematic error for R_b from lifetime, multiple, and shape double-tag measurements (in units of 10^{-3}). The sign is the sign of the correlation among the experiments. Adapted from Ref. 6.

The value of R_c has been determined using two different techniques. Both of the techniques take advantage of precise data available on the branching ratios for the various decay modes of charm hadrons. One of the methods is based on the measurement of leptons (μ and e) in hadronic events. The other method is based on reconstructed charm hadrons (primarily D^*).

Except for leptons produced in decays and conversions, leptons in hadronic events originate predominately from heavy-quark decays. Leptons from charmed hadrons can be separated from b hadrons on the basis momentum (p), and transverse momentum with respect to the jet axis (p_t). Using models of the rest frame momentum spectra of the b - and c -hadron decays, which are based on low-energy measurements, it is possible to predict the p and p_t spectra of the leptons at LEP energies. The value of R_c is extracted from a “grand” fit to the lepton p and p_t

spectrum which includes the branching ratio $Br(b \rightarrow \ell)$ and $Br(b \rightarrow c \rightarrow \ell)$ and the mean energy carried by primary b and c hadrons. In addition, these fits include the polar angle of the event thrust axis and the charge of the lepton, so that the charm and bottom forward-backward asymmetries and the average b-mixing parameter, $\bar{\chi}$, can be determined.

It is also possible to determine R_c from the measurement of reconstructed charm mesons. Most of the LEP measurements are based on the decay $D^{*\pm} \rightarrow D^0\pi^\pm$, where the D^0 is fully or partially reconstructed. The transition pion emitted in the $D^{*\pm}$ decay very closely follows the direction of the $D^{*\pm}$ because of the small Q value of the decay. This has two important consequences. First, the mass difference between the reconstructed D^* and reconstructed D^0 is small, even if some of the decay products of the D^0 are missing. Second, the transition pion very closely follows the jet-axis direction, allowing a charm signal to be isolated using only the transition pions p_t .

Since D^* mesons are also produced in the b-meson decay, information about the event shape, D^* decay length, and D^* momentum are all used to extract the fraction of D^* production due to $Z^0 \rightarrow c\bar{c}$. The largest external systematic error in this procedure comes from the uncertainty in the expected production of D^* in $Z^0 \rightarrow c\bar{c}$. This production rate has been taken from measurements in lower energy e^+e^- and has also been determined from double-tag techniques at LEP.

The OPAL double-tag technique uses an identified charm decay in one jet to produce a $Z^0 \rightarrow c\bar{c}$ sample, and then exploits the characteristic transverse momentum spectrum of the transition pions in the opposite jet to determine the inclusive branching ratio of $c \rightarrow D^{*\pm}$. There is good agreement between the parameters measured at LEP and those at lower energy. For example, the OPAL value of

$$Br(c \rightarrow D^*)Br(D^* \rightarrow D^0\pi)Br(D^0 \rightarrow K\pi) = (6.47 \pm 0.75) \times 10^{-3}$$

agrees with the value obtained at the low energy of

$$Br(c \rightarrow D^*)Br(D^* \rightarrow D^0\pi)Br(D^0 \rightarrow K\pi) = (7.1 \pm 0.5) \times 10^{-3}.$$

The DELPHI double-tag technique measurement uses a cut on the transverse momentum spectrum of the single particles to produce single and double tags in the same way as a decay length cut is used to produce single and double b-tagged samples.

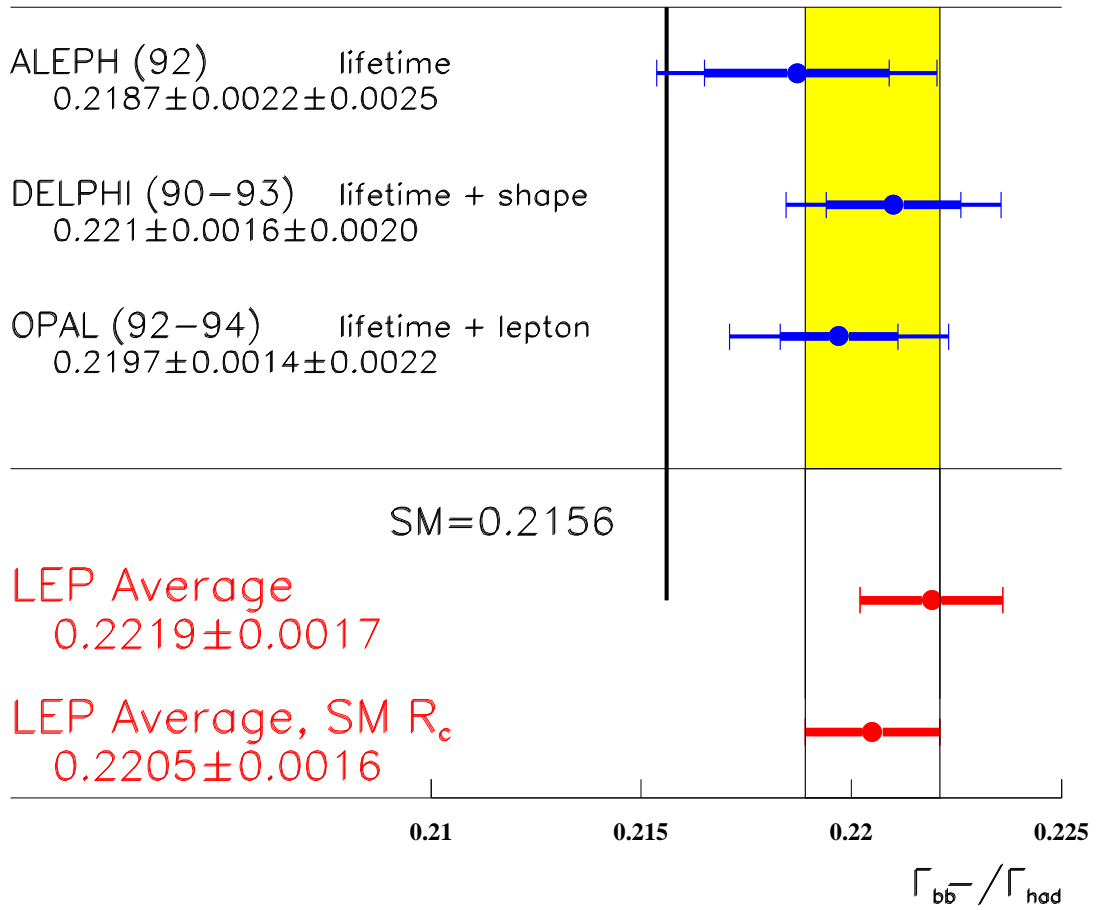


Figure 2: The individual measurements of R_b which dominate the average. The LEP average is shown with and without the Standard Model constraint of $R_c = 0.172$. The unconstrained average value incorporates the results of all of the heavy-flavor measurements and the LEP R_c analysis as described in the last portion of this section.

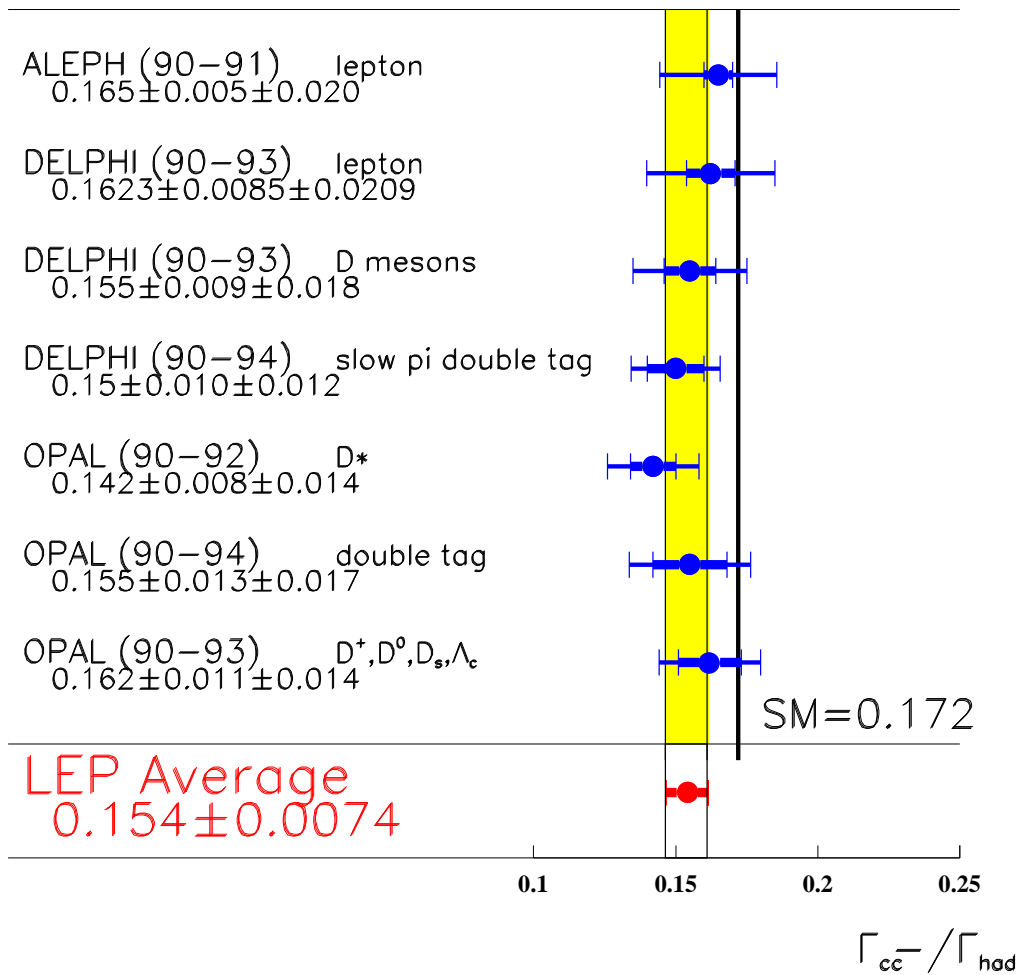


Figure 3: Individual measurements of R_c . The average value incorporates the results of the other LEP heavy flavor results as described in the last portion of this section.

The results of the measurements are summarized in Fig. 3. The resulting average value is somewhat smaller than the Standard Model prediction, and none of the individual measurements are larger than the Standard Model.

6.2 Heavy Quark Forward-Backward Asymmetries

The forward–backward asymmetry can be determined for $Z^0 \rightarrow b\bar{b}$ and $Z^0 \rightarrow c\bar{c}$ by tagging the events using methods similar to those employed for the measurement of R_b and R_c . To determine the direction of the event axis, three techniques are used: lepton charge, jet charge, and reconstruction of a charm hadron.

In measurements based on identified leptons in hadronic events, the sign of the lepton is used to infer the sign of the original quark. For example, a b quark will produce a b hadron, which will then decay to a negatively charged lepton, i.e., $b \rightarrow W^- c \rightarrow \ell^- \nu c$. Similarly, a c quark, which produces a c hadron, will then decay to a positively charged lepton. The measurement of the forward-backward asymmetry is complicated by both the mixing of neutral b mesons, which can cause the final state lepton to have the wrong sign, and the process $b \rightarrow c \rightarrow \ell^+$ which also produces a lepton of the wrong sign. Fortunately, both of these effects can be measured in the data. The average value of b mixing at LEP, $\bar{\chi}$, has been extracted from the relative number of same-sign and opposite-sign leptons in opposite hemispheres. (More details are given in Ref. 27.) The value of $Br(b \rightarrow c \rightarrow \ell^+)$ has similarly been extracted from the rate of opposite-signed leptons in the same hemisphere.

Leptons from $b \rightarrow \ell$ and $c \rightarrow \ell$ can be statistically separated from each other on the basis of p and p_t . The asymmetry is usually determined via a combined maximum likelihood fit to the p , p_t , and angular distribution of the data. These measurements depend on both the measured values of R_b and R_c as well as $\bar{\chi}$ and the assumed semileptonic branching ratios. The resulting correlations are all taken into account in determining the LEP average.

One of the disadvantages of the lepton-based technique is the relatively small branching ratio of b hadrons to leptons. In order to use tagging techniques based on lifetime, it is necessary to use jet charge to determine which jet is associated with the quark and which is associated with the antiquark. This method relies on a calculation of the average jet charge which is usually determined from a momentum-weighted average of the signs of charged tracks observed in a jet. The

momentum weighting exploits the fact that stiff tracks have a larger correlation with the sign of the quark charge than soft tracks.

At first sight, this method appears to depend completely on the Monte Carlo prediction of the reconstructed jet charge. However, the correlation between the charges of two jets (or hemispheres) can be measured to check the validity of the Monte Carlo. Similar methods that have been used for b-mixing studies are described elsewhere in these proceedings.²⁷

The forward-backward asymmetries of $Z^0 \rightarrow b\bar{b}$ and $Z^0 \rightarrow c\bar{c}$ can also be measured using events tagged with charm hadrons. Most measurements rely on the reconstructed charge of a D^* meson to deduce the charge of the initial heavy quark. Event shape, lifetime, and the momentum of the charm hadron are used to separate b- and c-quark final states. The reconstruction of the b asymmetry from the charm mesons utilizes the decay chain $b \rightarrow c \rightarrow D^{*\pm}$ to determine the direction of the jet axis.

6.3 Combined Fit

It is apparent from the discussion in this section that the results of the heavy-quark measurements are dependent on a common set of uncertainties which are both internal and external to the LEP electroweak measurements. To determine the LEP values, a χ^2 minimization technique is used where the internal parameters are determined directly and the external parameters (such as the charged multiplicities of D^+ decays and c- and b-hadron lifetimes) are allowed to vary within their measured constraints. Additional details about the LEP heavy-flavor fit can be found elsewhere.²⁸ The results of a four-parameter fit is

$$\begin{aligned}
 R_b &= 0.2219 \pm 0.0017 \\
 R_c &= 0.1543 \pm 0.0074 \\
 A_{FB}^{0,b} &= 0.0999 \pm 0.0031 \\
 A_{FB}^{0,c} &= 0.0725 \pm 0.0058,
 \end{aligned}
 \tag{21}$$

where the values of A_{FB} have been translated to the Z^0 pole and corrected for radiative QCD and QED effects. The Standard Model values of the γ exchange and $\gamma - Z$ have also been assumed. The measured values of R_b and R_c have a -0.34 correlation because of the dependence of the R_b measurement on R_c . While the values of forward-backward asymmetries are in agreement with the Standard Model prediction (see Fig. 4 and Table 10) which incorporates the Fermilab top

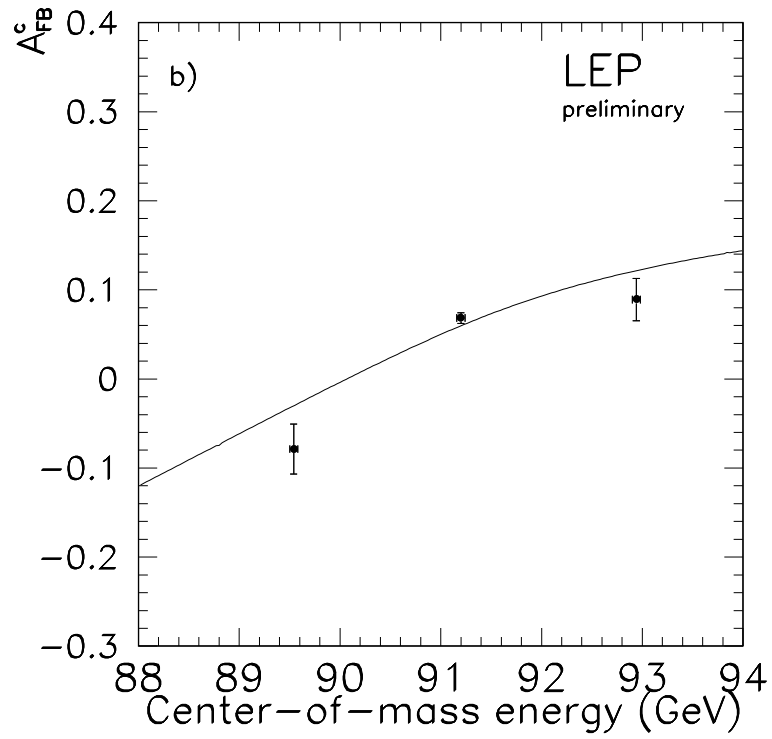
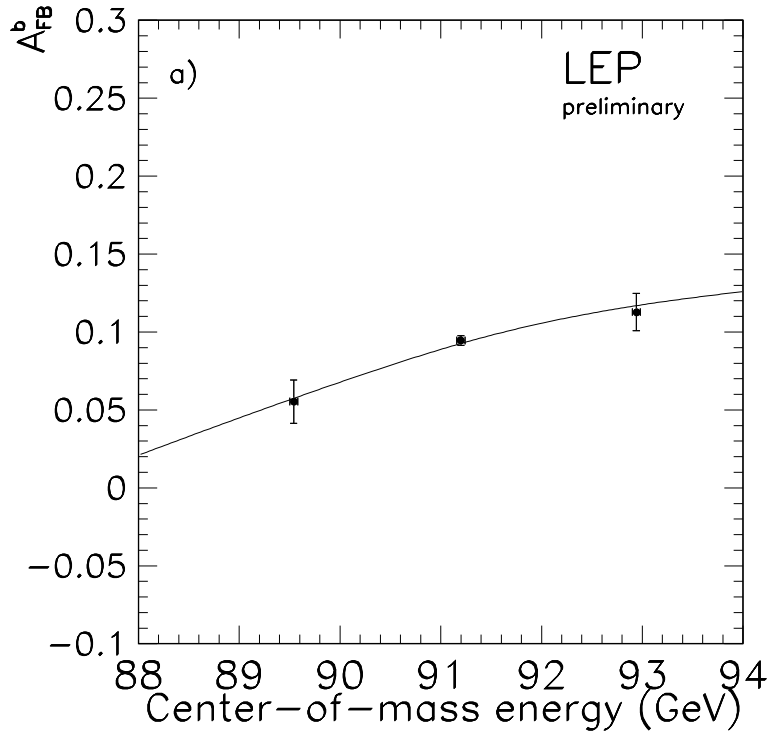


Figure 4: Forward-backward asymmetry for (a) $Z^0 \rightarrow b\bar{b}$ and (b) $Z^0 \rightarrow c\bar{c}$ as a function of center-of-mass energy. The curve shows the Standard Model prediction.

mass value of 180 ± 12 , the measured values of R_b and R_c do not agree with the Standard Model prediction, as can be seen from Fig. 5. If Gaussian errors are assumed, the LEP measurements only agree with the Standard Model at the 0.1% confidence level. Since the LEP measurements of R_b are dominated by systematic error, the assumption of Gaussian errors may not be justified. On the other hand, it is worth noting that it is difficult to obtain agreement with the Standard Model by adjusting only one of the quantities in Table 6. The largest common systematic error is due to uncertainties in the charm production and depends primarily on the production rate of the long-lived D^+ mesons in $Z^0 \rightarrow c\bar{c}$ events. This leads to a common uncertainty in the more precise measurements of R_b of approximately 0.001. To obtain agreement between the LEP measurements and the Standard Model, it would be necessary to change the production of D^+ by more than six times its uncertainty. Note that the D^+ rate depends primarily on the D^* rate production. This is because the decay $D^{*0} \rightarrow D^+\pi^-$ is not kinematically allowed, while the corresponding decay $D^{*+} \rightarrow D^0\pi^+$ occurs with a large branching ratio. We have already seen that the LEP measurements of the D^{*+} production are in good agreement with the lower energy measurements giving us confidence that the inputs to the R_b analysis have sensible values.

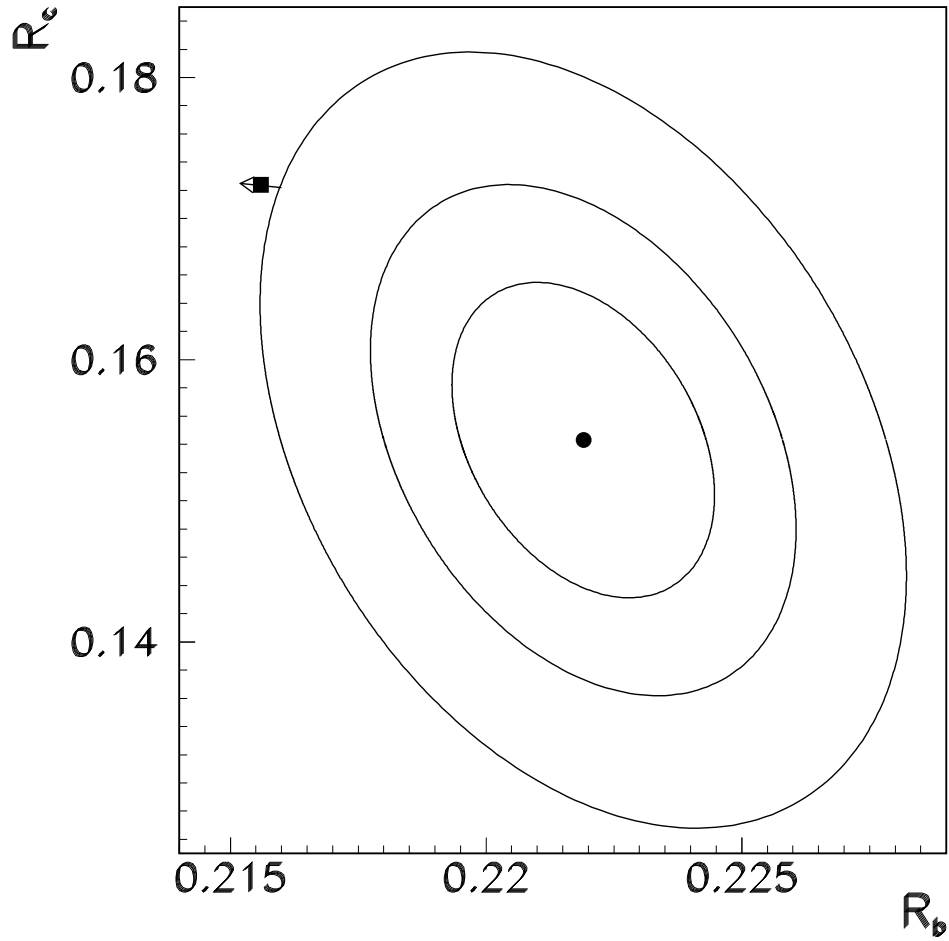


Figure 5: Contours in the R_b - R_c plane corresponding to 68%, 95%, and 99.9% confidence levels. The Standard Model prediction for $m_t = 180 \pm 12$ GeV is also shown. The arrow point shows the direction of increasing top mass.

7 Hadronic Forward-Backward Asymmetry

The jet-charge technique used in conjunction with the forward-backward asymmetry measurements discussed above can also be used to measure the hadronic forward-backward asymmetry averaged over quark flavors. These measurements are primarily sensitive to radiative corrections which affect the ratio of the vector to axial vector coupling of the electron. These measurements are reported in terms of the quantity $\sin^2\theta_{eff}^{lept}$ as defined in Eq. (5). Recall that the forward-backward asymmetry depends on the product $\mathcal{A}_e\mathcal{A}_f$ [see Eq. (11)]. For quark final states, most of the sensitivity radiative corrections come through \mathcal{A}_e which has a greater dependence on $\sin^2\theta_{eff}^{lept}$ than \mathcal{A}_f .

Experiment	$\sin^2\theta_{eff}^{lept}$
ALEPH ³³ '90-'93 prel.	$0.2323 \pm 0.0010 \pm 0.0010$
DELPHI ³⁴ '90-'91	$0.2345 \pm 0.0030 \pm 0.0027$
OPAL ³⁵ '91-'94 prel.	$0.2326 \pm 0.0012 \pm 0.0013$
Average	0.2325 ± 0.0013

Table 7: Summary of $\sin^2\theta_{eff}^{lept}$ measurements from the inclusive hadronic charge asymmetries at LEP. The first error is statistical, the second systematic. Adapted from Ref. 6.

The values of $\sin^2\theta_{eff}^{lept}$ determined using this technique are shown in Table 7. The systematic errors are dominated by the uncertainty in the hadronization process. A more complete discussion of the systematic errors which affect these measurements and the correlation of these errors with the jet-charge method used to determine $A_{FB}^{0,b}$ is given in Ref. 6.

8 Discussion and Combined Results

In this section, we combine the LEP measurements and compare them to the predictions of the Standard Model and the electroweak measurements made at the Tevatron and the SLC. We begin with a discussion of the lepton and quark couplings. Then all of the measurements are used to derive constraints on the top and Higgs masses.

8.1 Lepton Couplings

The axial and vector couplings of the leptons can be extracted from measurements of the lepton cross sections, the lepton asymmetries, and the tau polarization. The lepton cross sections are used to obtain the leptonic width,^{*} Γ_{l+l-} , which is related to the lepton couplings [Eq. (3)]. The other quantities are used to determine \mathcal{A}_f which is related to the lepton couplings [Eq. (12)].

The values derived from the LEP measurements⁶ are given in Table 8 and displayed in Fig. 6. There is good agreement between the LEP measurements and the Standard Model predictions which use the Tevatron top mass. The LEP values are also consistent with the constraint from \mathcal{A}_{LR} as measured by SLD,³⁹ which is also displayed in Fig. 6.

8.2 Neutrino Couplings

Decays of the Z^0 to neutrinos are not detected directly in the LEP detectors, making asymmetry measurements of these decays impossible. It is, however, possible to derive the quantity R_{inv} from the lepton cross section and the ratio R_ℓ . Taking

$$R_{inv} = \frac{\Gamma_{inv}}{\Gamma_{l+l-}} = \frac{\Gamma_Z - \Gamma_{had} - 3\Gamma_{l+l-}}{\Gamma_{l+l-}} \quad (22)$$

and using the relationship $\sigma_{ll}^{pole} = \frac{12\pi}{m_Z^2} \left(\frac{\Gamma_{l+l-}}{\Gamma_Z}\right)^2$, we have

$$R_{inv} = \left(\frac{12\pi}{m_Z^2} \frac{1}{\sigma_{ll}^{pole}}\right)^{\frac{1}{2}} - R_\ell - 3. \quad (23)$$

^{*}Note that the quantity $\sigma_{ll}^{pole} \equiv \frac{12\pi}{m_Z^2} \frac{\Gamma_{l+l-}^2}{\Gamma_Z^2}$ can be obtained from the LEP parameter set via the relationship $\sigma_{ll}^{pole} = \frac{\sigma_{had}^{pole}}{R_\ell}$.

	Without Lepton Universality
g_{ve}	-0.0368 ± 0.0017
$g_{v\mu}$	-0.0370 ± 0.0041
$g_{v\tau}$	-0.0371 ± 0.0018
g_{ae}	-0.50115 ± 0.00052
$g_{a\mu}$	-0.50113 ± 0.00076
$g_{a\tau}$	-0.50151 ± 0.00089
	Ratios of Couplings
$g_{v\mu}/g_{ve}$	1.01 ± 0.14
$g_{v\tau}/g_{ve}$	1.008 ± 0.071
$g_{a\mu}/g_{ae}$	1.0000 ± 0.0018
$g_{a\tau}/g_{ae}$	1.0007 ± 0.0020
	With Lepton Universality
$g_{v\ell}$	-0.0369 ± 0.0010
$g_{a\ell}$	-0.50119 ± 0.00041

Table 8: Results for the effective vector and axial vector couplings derived from the combined LEP data with and without the assumption of lepton universality. Adapted from Ref. 6.

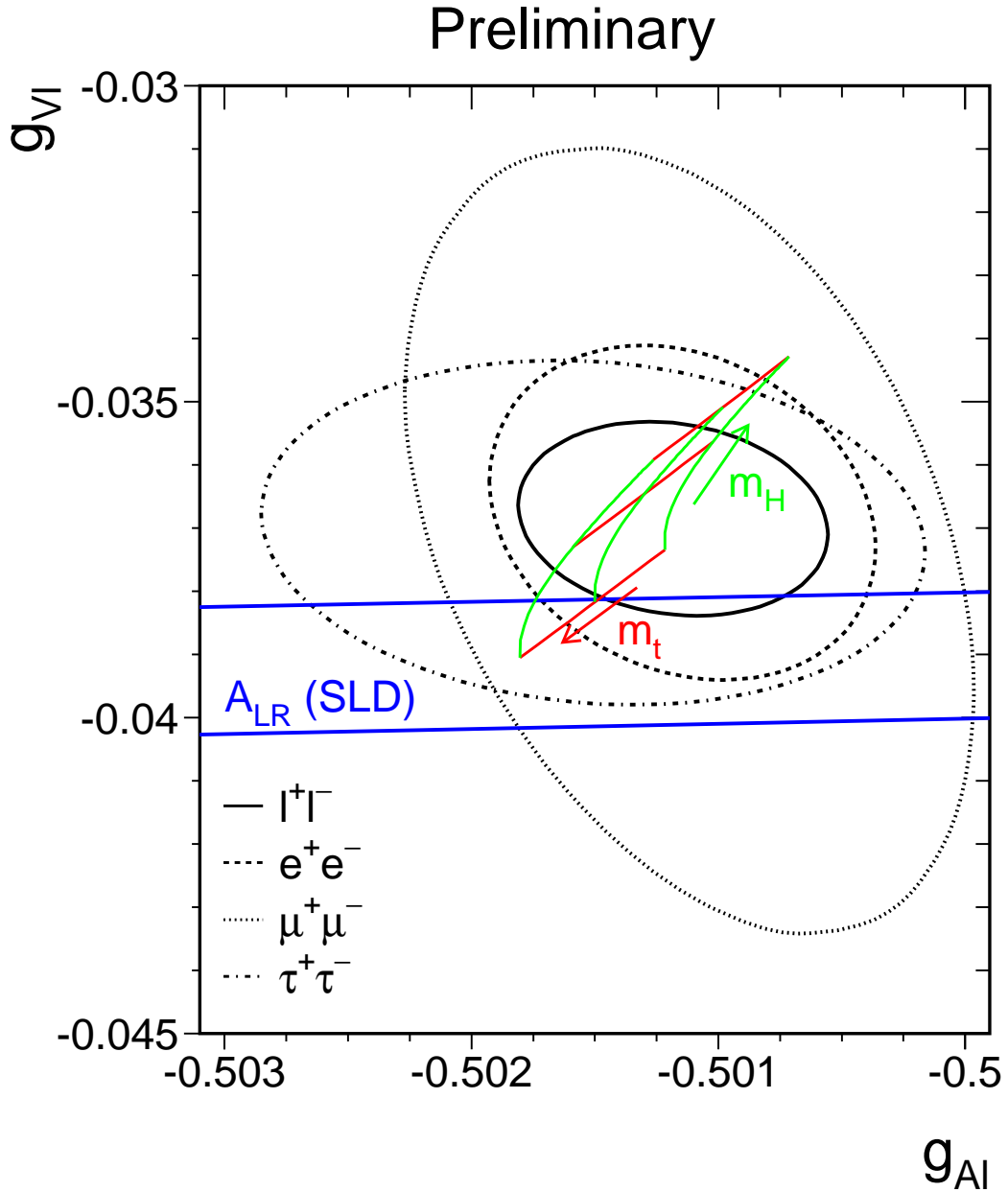


Figure 6: Contours of 68% probability in the $g_v - g_a$ plane for the preliminary LEP measurements. The constraint from the SLD \mathcal{A}_{LR} measurement appears as a band in the figure. The Standard Model prediction for $m_t = 180 \pm 12 \text{ GeV}$ and for $60 < m_H < 1000 \text{ GeV}$. The arrows point in the direction of increasing top and Higgs mass. Adapted from Ref. 6.

	LEP	SLD	Standard Model
\mathcal{A}_b	0.910 ± 0.037	0.841 ± 0.053	0.935
\mathcal{A}_c	0.660 ± 0.056	0.606 ± 0.090	0.667

Table 9: Comparison of LEP and SLD measurements with the Standard Model value of \mathcal{A}_b and \mathcal{A}_c . The Standard Model prediction is for a top mass of 178 GeV and a Higgs mass of 300 GeV.

Using the LEP line-shape data presented in Sec. 4,

$$R_{inv} = 5.956 \pm 0.031$$

is obtained. This is in good agreement with the Standard Model prediction of 5.973 ± 0.001 , where the small error on Standard Model prediction corresponds to $m_t = 180 \pm 12$ GeV and $60 < m_H < 1000$ GeV. Expressed as the number of neutrino generations which couple to the Z^0 , LEP obtains

$$N_\nu = 2.991 \pm 0.16.$$

To derive a constraint on the neutrino couplings, we assume that $g_{\nu\nu} = g_{\nu\nu} = g_\nu$ and obtain $g_\nu = +0.5011 \pm 0.0013$. The sign of g_ν is not determined from the LEP data and is taken from neutrino scattering measurements.³⁸

8.3 Quark Couplings

The couplings of b and c quarks to the Z^0 can be determined from the measurements of R_b and R_c as well as the heavy-quark forward-backward asymmetries. The measured values of the asymmetries depend on the product $\mathcal{A}_c\mathcal{A}_f$ [see Eq. (11)]. To find \mathcal{A}_f , we assume lepton universality and use the LEP lepton asymmetries and τ polarization. The resulting value is $\mathcal{A}_e = 0.1464 \pm 0.0039$. The values of the LEP measurement are compared to the Standard Model prediction in Table 9. Also shown in the table are the measurements of \mathcal{A}_b and \mathcal{A}_c made by SLD using the forward–backward polarized asymmetries.³⁶

It is possible to derive the quark couplings by adding the constraint provided by the measurement of R_b and R_c . We convert R_b and R_c to partial widths using the hadronic width of the Z^0 derived from the line-shape fit of 1744.8 ± 3.0 GeV.

In addition, the world average value³⁷ of $\alpha_s = 0.117 \pm 0.006$ is used to compute the QCD corrections. The resulting contours are shown in Fig. 7.

8.4 Top and Higgs Mass

All of the LEP electroweak observables presented above can be used in a fit to determine, in the context of the Standard Model, the values of α_s and m_t . The values of the quantities input to the fit are shown in Table 10 as well as the Standard Model values for the quantities. The result of the fit is

$$\begin{aligned} m_t &= 170 \pm 10 \quad {}^{+17}_{-10} \quad GeV \\ \alpha_s &= 0.125 \pm 0.004 \pm 0.002, \end{aligned}$$

where the χ^2 is 18 for nine degrees of freedom. The central value is for $m_H = 300$ GeV, and the second error reflects the variation in the result as the Higgs mass is varied in the interval $60 < m_H < 1000$ GeV. The LEP value is in excellent agreement with the direct determination of $m_t = 180 \pm 12$ GeV made at the Tevatron. The value of α_s is slightly higher than the world average, adjusted to remove input from the Z^0 line shape, of 0.117 ± 0.006 (Ref. 37). The poor quality of the χ^2 is primarily due to the large discrepancy between the measured value of R_b , R_c , and the Standard Model prediction. Recall that R_b has only a moderate dependence on the top mass and R_c is almost independent of the top mass. As a result, refitting without R_b and R_c increases the value obtained for the top mass by only 4 GeV.

The dependence of the m_t prediction on the assumed Higgs mass shows that the LEP measurements will have some sensitivity to the Higgs mass if an external measurement of m_t is added to the fit. Combining the LEP measurements with the Tevatron top-mass measurement^{1,2} of $m_t = 180 \pm 12$ GeV, the change in χ^2 , $\Delta\chi^2$, as a function of Higgs mass, reveals the logarithmic dependence of the electroweak observables to the Higgs mass as shown in Fig. 8.

We can improve our estimate of the Higgs mass by including the electroweak measurements made at SLD with polarized beams,³⁹ the value of $1 - m_W^2/m_Z^2$ from neutrino scattering,⁴⁰⁻⁴² and the Tevatron W mass determination⁴³ summarized in Table 11. Adding these constraints to the Standard Model fit, $m_t = 178 \pm 8_{-20}^{+17}$ GeV and $\alpha_s = 0.123 \pm 0.004 \pm 0.002$ for $m_H = 300$ GeV are obtained. Figure 8 also shows the $\Delta\chi^2$ curves for the full electroweak set. The combined data favor relatively low values of the Higgs mass, but the data is not yet precise

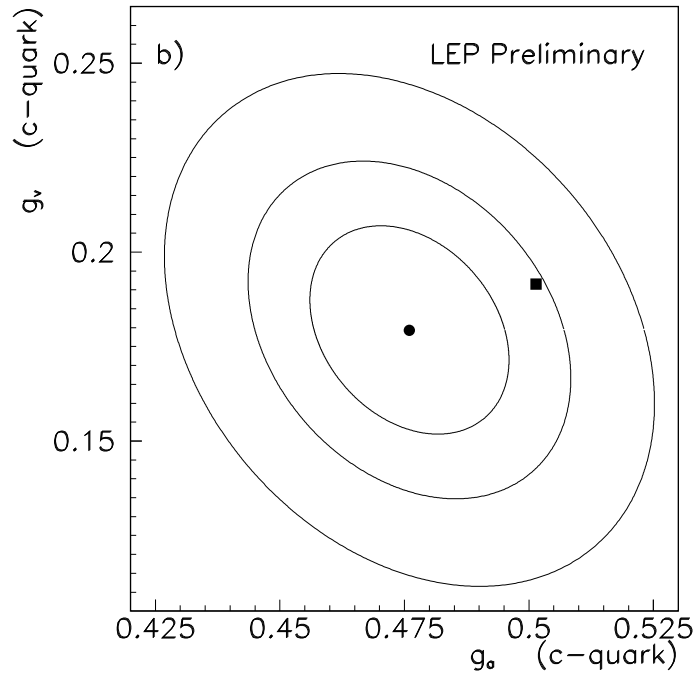
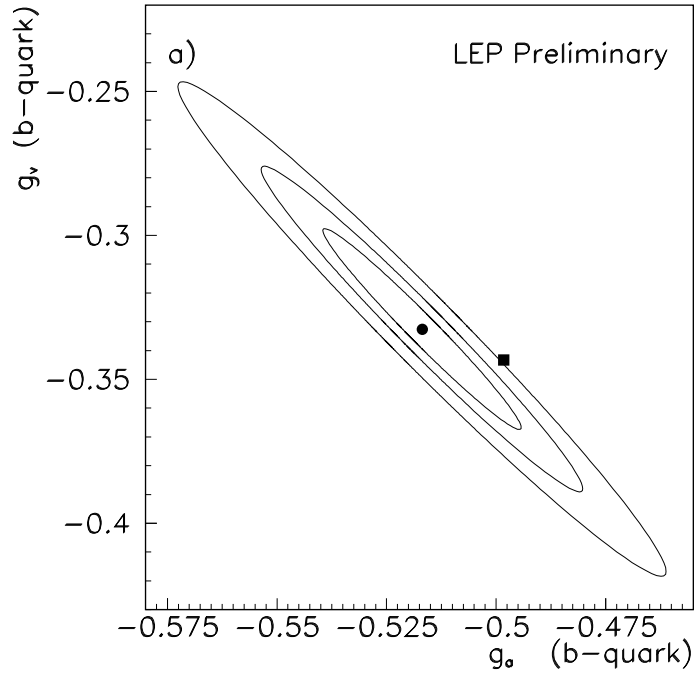


Figure 7: Contours of 68%, 95%, and 99.9% probability in the $g_v - g_a$ plane for the preliminary LEP measurements of (a) b-quark couplings and (b) c-quark couplings. The solid square shows the Standard Model prediction for $m_t = 180$ GeV and $m_H = 300$ GeV.

enough as to exclude a Standard Model Higgs at the upper range of its allowed value. At LEP, direct searches for the Standard Model Higgs have excluded it in the mass region below 60 GeV (Ref. 44).

The measurement of the Γ_Z , R_ℓ , and σ_{had}^{pole} provide additional constraints on possible deviation in R_b and R_c from physics beyond the Standard Model. One way to use these constraints is to allow for an additional contribution to $\Gamma_{b\bar{b}}$ by taking $\Gamma_{b\bar{b}} = \Gamma_{b\bar{b}}^{SM} + \Delta_{b\bar{b}}$. Fitting to all of the data, $\Delta_{b\bar{b}} = 11.7 \pm 3.8 \pm 1.4$ MeV with $m_t = 181 \pm 8_{-19}^{+17}$ GeV and $\alpha_s = 0.102 \pm 0.008$ is obtained. The resulting value of α_s is in agreement with the world average, but much lower than the value obtained from the line-shape measurements reported above. Allowing for deviation in $\Delta_{c\bar{c}}$ in $\Gamma_{c\bar{c}}$, a value of $\alpha_s = 0.18 \pm 0.04$ is obtained. This value of α_s is only consistent with the world average at the two standard-deviation level.

	Measurement	Standard Model Fit	Pull
line-shape and lepton asymmetries:			
m_Z [GeV]	91.1884 ± 0.0022	91.1882	0.1
Γ_Z [GeV]	2.4963 ± 0.0032	2.4973	-0.3
σ_{had}^{pole} [nb]	41.488 ± 0.078	41.450	0.5
R_ℓ	20.788 ± 0.032	20.773	0.5
$A_{FB}^{0,\ell}$	0.0172 ± 0.0012	0.0159	1.1
τ polarization:			
\mathcal{A}_τ	0.1418 ± 0.0075	0.1455	-0.5
\mathcal{A}_e	0.1390 ± 0.0089	0.1455	-0.7
b and c quark results:			
$R_b^{(a)}$	0.2219 ± 0.0017	0.2156	3.7
$R_c^{(a)}$	0.1543 ± 0.0074	0.1724	-2.5
$A_{FB}^{0,b(a)}$	0.0999 ± 0.0031	0.1020	-0.7
$A_{FB}^{0,c(a)}$	0.0725 ± 0.0058	0.0728	0.0
$q\bar{q}$ charge asymmetry:			
$\sin^2\theta_{eff}^{lep} (\langle Q_{FB} \rangle)$	0.2325 ± 0.0013	0.23172	0.6

Table 10: The LEP measurements used in the combined Standard Model fit for m_t and α_s . The Standard Model fit results and the pulls (difference between measurement and fit in units of the measurement error) are derived from the fit including data from the Tevatron and SLD for a fixed value of $m_H = 300$ GeV. The full fit includes the correlation matrices given in Ref. 6.

	Measurement	Standard Model Fit	Pull
(a) <u>SLD</u>			
$\sin^2\theta_{eff}^{lept} (\mathcal{A}_{LR})$ [Ref. 39]	0.23049 ± 0.00050	0.23172	-2.5
R_b [Ref. 36]	0.2171 ± 0.0054	0.2156	0.3
\mathcal{A}_b [Ref. 36]	0.841 ± 0.053	0.935	-1.8
\mathcal{A}_c [Ref. 36]	0.606 ± 0.090	0.667	-0.7
(b) <u>$p\bar{p}$ and νN</u>			
m_W [GeV] ($p\bar{p}$) [Ref. 43]	80.26 ± 0.16	80.35	-0.5
$\sin^2\theta_W$ (νN) [Ref. 40–42]	0.2257 ± 0.0047	0.2237	0.4

Table 11: (a) SLD results for $\sin^2\theta_{eff}^{lept}$ from the measurement of the left-right polarization asymmetry, for R_b and for \mathcal{A}_b and \mathcal{A}_c from polarized forward-backward asymmetries. (b) Electroweak precision tests from $p\bar{p}$ colliders and νN -scattering. Correlations between the systematic errors of the SLD heavy-quark measurements and of the LEP measurements have been included in the fit. Adapted from Ref. 6.

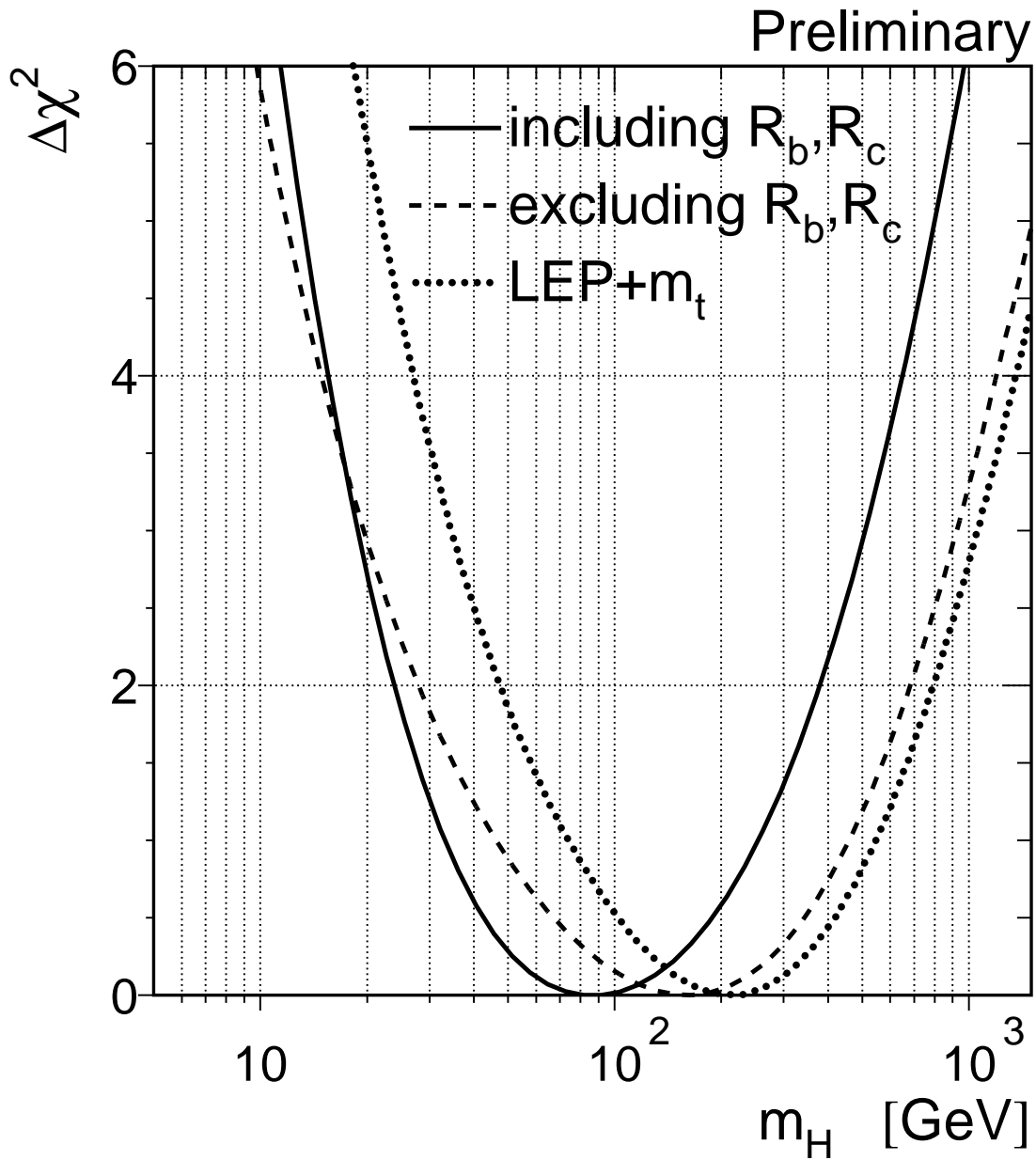


Figure 8: Sensitivity of the electroweak observables to the Higgs mass for LEP and m_t and for all electroweak data. The latter result is also shown when R_b and R_c are excluded from the fit. Note that $\Delta\chi^2$ is plotted.

9 Conclusion and Outlook

Almost all of the precision electroweak measurements which have been made at LEP I are in excellent agreement with the predictions of the Standard Model and the recent measurement of the top-quark mass by DØ (Ref. 2) and CDF (Ref. 1). The preliminary measurements of R_b and R_c , however, show a marked departure from the prediction of the Standard Model.

Improvement in the statistical and systematic errors on many of the measurements presented here can be expected as the LEP experiments complete the final analysis of the 1994 data. Improvements in the statistical errors on R_b and R_c are expected as two of the LEP experiments have not yet analyzed the large amount of data delivered in 1994. Improvements in the systematic errors on these quantities can also be expected as the experiments endeavor to reduce the dependence of their measurements on external measurements, and as the external measurements become more precise.

Data from the 1995 run, the last LEP run at the Z^0 , are presently being analyzed. Because of the additional data taken off the Z^0 peak, the addition of the 1995 data will improve our knowledge of Γ_Z .

Starting in the Fall of 1995, LEP will begin running well above the Z^0 at $\sqrt{s} \sim 140$ GeV. In 1996, it is hoped that the W threshold will be reached and a first measurement of the W mass can be made. One goal of the LEP II physics program is to acquire sufficient data to make a measurement of the W mass at the 40 MeV level.

Another contribution of LEP II to electroweak measurements will be to extend the reach of the Higgs search from the present limit near 60 GeV to m_Z or higher, depending on the final center-of-mass energy of the LEP II machine.⁴⁴

Acknowledgments

I would like to thank the LEP Collaborations ALEPH, DELPHI, L3, and OPAL for making their latest physics results available in time for the SLAC Summer Institute. I received invaluable assistance from D. Schaile and P. Wells in making the combined fits which were presented at the Institute. In this report, I have included a few results which were not available in time for the Institute. I have relied heavily on the work of the LEP Electroweak Working Group which is sum-

marized in Ref. 6. I would also like to thank the organizers of the Institute for providing a well-organized and stimulating program.

References

- [1] CDF Collaboration, F. Abe *et al.*, Phys. Rev. Lett. **74**, 2626 (1995).
- [2] DØ Collaboration, S. Abachi *et al.*, Phys. Rev. Lett. **74**, 2632 (1995).
- [3] M. Swartz, these proceedings.
- [4] S. Eidelmann and F. Jegerlehner, *Hadronic Contributions to $(g-2)$ of the Leptons and to the Effective Fine Structure Constant $\alpha_{em}(m_Z^2)$* , PSI-PR-95-1, BUDKERINP 95-5, JANUARY 1995.
- [5] M. Consoli and W. Hollik, *Z Physics at LEP 1*, CERN 89-08, edited by G. Altarelli *et al.*, Vol. 1 (1989), p. 7.
- [6] The LEP Collaborations, *A Combination of Preliminary LEP Electroweak Measurements and Constraints on the Standard Model*, CERN-PPE/95-172.
- [7] LEP energy working group, R. Asmann *et al.*, Z. Phys C **66**, 567 (1995).
- [8] ALEPH Collaboration, D. Decamp *et al.*, Z. Phys. C **48**, 365 (1990);
ALEPH Collaboration, D. Decamp *et al.*, Z. Phys. C **53**, 1 (1992);
ALEPH Collaboration, D. Decamp *et al.*, Z. Phys. C **60**, 71 (1993);
ALEPH Collaboration, D. Decamp *et al.*, Z. Phys. C **62**, 539 (1994);
ALEPH Collaboration, D. Decamp *et al.*, *Preliminary Results on Z Production Cross-Sections and Lepton Forward-Backward Asymmetries Using the 1994 Data*, **eps0398**.
- [9] DELPHI Collaboration, P. Aarnio *et al.*, Nucl. Phys. B **367**, 511 (1991);
DELPHI Collaboration, P. Abreu *et al.*, Nucl. Phys. B **417**, 3 (1994);
DELPHI Collaboration, P. Abreu *et al.*, Nucl. Phys. B **418**, 403 (1994);
DELPHI Collaboration, DELPHI, Note 95-62 PHYS 497, July 1995.
- [10] L3 Collaboration, B. Adeva *et al.*, Z. Phys. C **51**, 179 (1991);
L3 Collaboration, O. Adriani *et al.*, Phys. Rep. **236**, 1 (1993);
L3 Collaboration, M. Acciarri *et al.*, Z. Phys. C **62**, 551 (1994);
L3 Collaboration, L3 Note 1809, July 1995.
- [11] OPAL Collaboration, G. Alexander *et al.*, Z. Phys. C **52**, 175 (1991);
OPAL Collaboration, P. D. Acton *et al.*, Z. Phys. C **58**, 219 (1993);
OPAL Collaboration, R. Akers *et al.*, Z. Phys. C **61**, 19 (1994);
OPAL Collaboration, OPAL Internal Physics Note PN142, July 1994;
OPAL Collaboration, OPAL Internal Physics Note PN166, February 1995.
- [12] S. Jadach *et al.*, Phys. Lett. B **353**, 362 (1995).
- [13] D. Bardin *et al.*, Z. Phys. C **44**, 493 (1989);
D. Bardin *et al.*, Comp. Phys. Comm. **59**, 303 (1990);
D. Bardin *et al.*, Nucl. Phys. B **351**, 1 (1991);
D. Bardin *et al.*, Phys. Lett. B **255**, 290 (1991);
D. Bardin *et al.*, CERN-TH 6443/92 (May 1992).
- [14] ALEPH Collaboration, "Improved tau polarisation measurements," submitted to Z. Phys., CERN-PPE/95-023 (1995).

- [15] DELPHI Collaboration, P. Abreu *et al.*, Z. Phys. C **67**, 183 (1995).
- [16] L3 Collaboration, O. Accaiari *et al.*, Phys. Lett. B **341**, 24 (1994);
L3 Collaboration, *A Preliminary Update of \mathcal{A}_τ and \mathcal{A}_e Using the 1994 Data*, L3 Note 1793, July 5, 1995.
- [17] OPAL Collaboration, *Updated Measurement of the Tau Polarisation Asymmetries*, OPAL Internal Physics Note PN172, March 1995.
- [18] P. Dornan, these proceedings.
- [19] ALEPH Collaboration, D. Buskulic *et al.*, Phys. Lett. B **313**, 549 (1993).
- [20] ALEPH Collaboration, D. Buskulic *et al.*, Phys. Lett. B **313**, 535 (1993).
- [21] DELPHI Collaboration, “Measurement of the partial decay width $R_b = \Gamma_{b\bar{b}}/\Gamma_{had}$ with the DELPHI detector at LEP,” contributed paper to EPS-HEP-95 Brussels, **eps0570**.
- [22] L3 Collaboration, O. Adriani *et al.*, Phys. Lett. B **307**, 327 (1993).
- [23] OPAL Collaboration, Z. Phys. C **67**, 17 (1995);
OPAL Collaboration, “An update of the measurement of $\Gamma_{b\bar{b}}/\Gamma_{had}$ using a double tagging method,” contributed paper to EPS-HEP-95, **eps0278**.
- [24] ALEPH Collaboration, D. Buskulic *et al.*, Z. Phys. C **62**, 179 (1994).
- [25] DELPHI Collaboration, “Study of charm mesons production in Z^0 decays and measurement of Γ_c/Γ_h ,” contributed paper to EPS-HEP-95, **eps0557**.
- [26] OPAL Collaboration, R. Akers *et al.*, Z. Phys. C **62**, 27;
OPAL Collaboration, “A measurement of $b(c \rightarrow D^*)$ and $\Gamma_{c\bar{c}}/\Gamma_{had}$ using a double tagging technique,” contributed paper to EPS-HEP-95 Brussels, **eps0289**;
OPAL Collaboration, *A Summary of OPAL Measurements of Charm Production in Z Decays*, OPAL Physics Note PN190.
- [27] P. Dornan, these proceedings.
- [28] LEP Electroweak Working Group, *Combination of Heavy Flavour Electroweak Measurements at LEP*, in preparation, to be submitted to Nucl. Instrum. Methods.
- [29] ALEPH Collaboration, D. Buskulic *et al.*, Z. Phys. C **26**, 179 (1994);
ALEPH Collaboration, D. Buskulic *et al.*, Phys. Lett. B **335**, 99 (1994);
ALEPH Collaboration, D. Buskulic *et al.*, Z. Phys. C **62**, 1 (1994);
ALEPH Collaboration, “ $B^0\bar{B}^0$ mixing and $b\bar{b}$ asymmetry from high- $p - t$ leptons,” ALEPH 94-036, contributed paper to the LaThuile and Moriond Winter conferences, 1994;
ALEPH Collaboration, *Heavy Flavour Lepton Contribution for Summer 1994 Conferences*, ALEPH 94-123 PHYSICS 94-107;
ALEPH Collaboration, “Measurement of the semileptonic b branching ratios from inclusive leptons in Z decays,” contributed paper to EPS-HEP-95 Brussels, **eps0404**;
ALEPH Collaboration, “The forward-backward asymmetry for charm quarks at the Z pole: An update,” contributed paper to EPS-HEP-95 Brussels, **eps0634**.
- [30] DELPHI Collaboration, P. Abreu *et al.*, Z. Phys C **65**, 569 (1995);
DELPHI Collaboration, P. Abreu *et al.*, Z. Phys C **66**, 341 (1995);
DELPHI Collaboration, “Measurement of the forward-backward asymmetries

- of $e^+e^- \rightarrow Z \rightarrow b\bar{b}$ and $e^+e^- \rightarrow Z \rightarrow c\bar{c}$,” contributed paper to EPS-HEP-95 Brussels, **eps0571**.
- [31] L3 Collaboration, O. Adriani *et al.*, Phys. Lett. B **292**, 454 (1992);
 L3 Collaboration, M. Acciarri *et al.*, Phys. Lett. B **335**, 542 (1994);
 L3 Collaboration, *Measurement of R_b and $BR(b \rightarrow lX)$ from b -Quark Semileptonic Decays*, L3 Note 1449, July 1993;
 L3 Collaboration, *L3 Results on $A_{FB}^{0,b}$, $A_{FB}^{0,c}$, and χ for the Glasgow Conference*, L3 Note 1624;
 L3 Collaboration, *L3 Results on R_b and $BR(b \rightarrow l)$ for the Glasgow Conference*, L3 Note 1625.
- [32] OPAL Collaboration, R. Akers *et al.*, Z. Phys. C **60**, 199 (1993);
 OPAL Collaboration, R. Akers *et al.*, Z. Phys. C **67**, 365 (1995);
 OPAL Collaboration, “Measurement of the forward-backward asymmetries of and $e^+e^- \rightarrow Z \rightarrow b\bar{b}$ and $e^+e^- \rightarrow Z \rightarrow c\bar{c}$ from events tagged by a lepton, including 1994 data,” contributed paper to EPS-HEP-95 Brussels, **eps0279**;
 OPAL Collaboration, “A measurement of the charm and bottom forward-backward asymmetry using D mesons with the OPAL detector at LEP,” contributed paper to EPS-HEP-95 Brussels, **eps0290**.
- [33] ALEPH Collaboration, D. Decamp *et al.*, Phys. Lett. B **259**, 377 (1991);
 ALEPH Collaboration, ALEPH-NOTE 93-041 PHYSIC 93-032 (1993);
 ALEPH Collaboration, ALEPH-NOTE 93-042 PHYSIC 93-044 (1993);
 ALEPH Collaboration, ALEPH-NOTE 93-044 PHYSIC 93-036 (1993);
 ALEPH Collaboration, “*Jet charge measurements in $Z \rightarrow q\bar{q}$ decays*,” contributed paper to EPS-HEP-95 Brussels, **eps0449**.
- [34] DELPHI Collaboration, P. Abreu *et al.*, Phys. Lett. B **227**, 371 (1992).
- [35] OPAL Collaboration, P. D. Acton *et al.*, Phys. Lett. B **294**, 436 (1992);
 OPAL Collaboration, OPAL Physics Note PN195 (1995).
- [36] R. Messner, these proceedings.
- [37] S. Bethke, “Status of α_s measurements,” XXXth Rencontres de Moriond, QCD and Hadronic Interactions, Les Arcs, March 19-26, 1995.
- [38] CHARM II Collaboration, P. Viliain *et al.*, Phys. Lett. B **335**, 246 (1994).
- [39] T. Schalk, these proceedings.
- [40] CDHS Collaboration, H. Abramowicz *et al.*, Phys. Rev. Lett. **57**, 446 (1986);
 CDHS Collaboration, A. Blondel *et al.*, Z. Phys. C **45**, 351 (1990).
- [41] CHARM Collaboration, J. V. Allaby *et al.*, Phys. Lett. B **177**, 446 (1986);
 CHARM Collaboration, J. V. Allaby *et al.*, Z. Phys. C **36**, 611 (1987).
- [42] CCFR Collaboration, C. G. Arroyo *et al.*, Phys. Rev. Lett. **72**, 3452 (1994);
 D. Harris, *CCFR Measurement of R_ν and a New Extraction of $\sin^2 \theta_W$* , EPS-HEP-95 Conference, Brussels.
- [43] R. Hughes and N. Hadley, these proceedings.
- [44] J.-F. Grivaz, “New particle searches,” presented at the EPS-HEP-95 Conference, LAL 95-83.